Journal of Food Engineering 120 (2014) 197–203

Contents lists available at ScienceDirect

Journal of Food Engineering

journal homepage: www.elsevier.com/locate/jfoodeng

Influence of dielectric properties on the heating rate in free-running oscillator radio frequency systems

Yang Jiao [a], Juming Tang [a,*], Shaojin Wang [a,b], Tony Koral [c]

[a] Department of Biological Systems Engineering, Washington State University, Pullman, WA 99164-6120, USA
[b] College of Mechanical and Electronic Engineering, Northwest A&F University, Yangling, Shaanxi 712100, China
[c] Koral Associates, Goring Road, Woodcote, South Oxfordshire, RG8 0QE, United Kingdom

ARTICLE INFO

Article history:
Received 4 February 2013
Received in revised form 30 May 2013
Accepted 25 July 2013
Available online 6 August 2013

Keywords:
Dielectric properties
Radio frequency
Heating rate
Mathematical modeling

ABSTRACT

The heating behavior of a food product in a radio frequency (RF) heater with a free-running oscillator largely depends on the dielectric properties of the food material in processing. In this study, heating rate was mathematically derived as a function of its influencing factors in a RF system. This relationship was validated by experiments using conditioned salt solutions and peanut butter samples in a 27.12 MHz, 6 kW RF system. The dielectric properties of the materials used to validate the model ranged from 3.3 to 91.6 for dielectric constant and from 0.1 to 1577.0 for dielectric loss factor. The comparison between theoretical and experimental results showed a good agreement for the tested samples. Both dielectric constant and loss factor influenced the heating rate under a fixed electrode gap and frequency. When the values of dielectric constant and loss factor were close to one another, the maximum heating rate can be reached.

1. Introduction

Radio frequency (RF) is an electromagnetic wave with a frequency range of 3 kHz to 300 MHz. The US Federal Communications Commission (FCC) allocates 13.56, 27.12 and 40.68 MHz in the RF range for industrial, scientific and medical (ISM) application (Wang and Tang, 2001). RF heating has been applied in the food industry as an efficient dielectric heating method for years. Because of its volumetric heating, adjustable heating rate and high energy efficiency, RF heating is already showing its advantages in thawing and in conditioning of biscuit post baking (Farag et al., 2011; Palazoglu et al., 2012). Wide applications have also been explored in disinfestation, enzyme inactivation, pasteurization and sterilization (Rice, 1993; Wang et al., 2003b,2010; Luechapattanaporn et al., 2005; Guo et al., 2006, 2011; Manzocco et al., 2008). The 50 ohm technology and free-running oscillators are two different designs of RF heating systems. Although 50 ohm systems use modern methods to control the frequency and power, the free-running oscillator design is still the most commonly used in the food industry because of the low cost, simple structure and flexibility. In a free-running oscillator RF heater, the portion of power converted to useful heat depends mainly on the properties of the material (Rowley, 2001).

For a free-running oscillator RF system, "parallel plates" are the most commonly used electrode configuration for bulk material heating (Jones and Rowley, 1996). The food material is placed in-between the two parallel plate electrodes of the applicator, which act as a capacitor. When energized, the generator provides high voltage, high frequency power to the electrodes in the applicator, and the food material with certain dielectric properties is heated up in the high density alternating electric field. In dielectric heating, the dielectric properties of food products are important intrinsic properties that directly influence the energy conversion rate. The complex dielectric property ε^* is the sum of the real part – dielectric constant ε', and the imaginary part – loss factor ε''. Due to the nature of the free-running oscillator RF system, the dissipated power could not be measured directly because of the varying voltage and electric field. Therefore, the only way to estimate the dissipated power in food is to calculate from theoretical equations. The power conversion in the material is described as (Choi and Konrad, 1991):

$$P = 2\pi f \varepsilon_0 \varepsilon'' |\overrightarrow{E_m}|^2 \quad (1)$$

where P is the power conversion in food material from electromagnetic to thermal energy, (W/m^3); f is the frequency of the RF generator, (Hz); ε_0 is the permittivity of vacuum (8.854×10^{-12} F/m); ε'' is the loss factor of the material; $\overrightarrow{E_m}$ is the electric field intensity in the food sample (V/m) (Fig. 1).

* Corresponding author. Tel: +1 509 335 2140; fax: +1 509 335 2722.
E-mail address: jtang@wsu.edu (J. Tang).

0260-8774/$ - see front matter © 2013 Elsevier Ltd. All rights reserved.
http://dx.doi.org/10.1016/j.jfoodeng.2013.07.032

The dielectric properties of various food materials over the RF frequency band have been reported over the past 40 years (To et al., 1974; Nelson, 1981; Calay et al., 1994; Sosa-Morales et al., 2010). The dielectric properties are usually functions of temperature, frequency, density, moisture content, and other compositions of the food. Thus, for a given material, the dielectric properties may vary during heating, and the heating behavior may also change accordingly. Therefore, knowing the dielectric properties as a function of temperature, moisture content and other properties before running experiments may help to predict possible thermal run away and temperature distribution in the bulk food.

It has been a general belief that the power absorption in food is positively related to the loss factor of a food material (Piyasena et al., 2003). However, Birla et al. (2008a) found that in a free-running oscillator RF system, the maximum heating rate was reached when the loss factor of a load is 180 in the studied range between 80 and 350. But the conclusion was derived through theoretical analysis without experimental validation. Wang et al. (2008) reported a reverse relationship between ε'' and heating rate in mashed potato samples of different salt contents based on both experimental and simulation results. A theoretical equation was developed to explain the phenomena, but the simple assumptions in this study limited its application only to a narrow range of dielectric properties, i.e.: ε': 83.3–84.7; ε'': 78.7–173.2. Tiwari et al. (2011a) conducted a computer simulation on RF heating of dry food with COMSOL Multiphysics® software to analyze the influence of dielectric properties on power distribution. In their results, the maximum power distribution and better heating uniformity were reached when the values of dielectric constant and loss factor were small and comparable. But no adequate explanation was given for this phenomenon. So far, there is no systematic research showing in details how the dielectric properties influence heating behavior in free-running oscillator RF systems.

The general goal of this study was to better understand the influence of dielectric properties on RF heating, and further assist experiment design to guide the development of industrial RF heating processes. The specific objectives of this study were to: (1) theoretically analyze the influencing factors of RF heating rate, and use a mathematical model to estimate the heating rate as a function of material properties for a given condition of a RF heater; (2) validate the mathematical model with salty water when only dielectric loss factor changes as a function of salt concentration; and (3) validate the model with conditioned peanut butter samples when both dielectric constant and loss factor change as a function of moisture content and temperature.

2. Materials and methods

2.1. Theoretical model

The power conversion in a food material during RF heating depends on the working frequency, loss factor and the electric field density inside the material (Birla et al., 2008b). When heat loss to the ambient is negligible, the heating rate in a food after absorbing RF power can be described as:

$$P = \rho c_p \frac{\partial T}{\partial t} = 2\pi f \varepsilon_0 \varepsilon'' |\overrightarrow{E_m}|^2 \tag{2}$$

where ρ is the density of the load, (kg/m^3); c_p is the heat capacity of the load, (J/kg K); $\partial T/\partial t$ is the transient heating rate of the load during RF heating (°C/s).

When air is the only surrounding media between the electrodes other than the food sample, the continuity boundary condition of the electric flux density can be applied at the interface of the load and air for a simplified case shown in Fig. 1 (Metaxas, 1996; Birla et al., 2008a,b). The continuity equation can be written as:

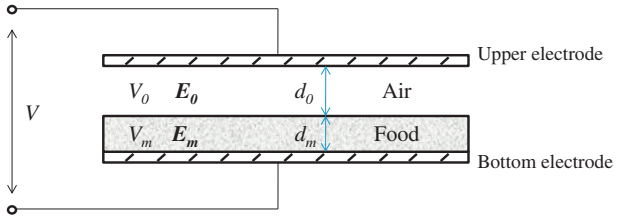

Fig. 1. Scheme of RF heating system with parallel plate electrodes.

$$\overrightarrow{D_n} = \varepsilon_0 \overrightarrow{E_0} = \varepsilon_0 \varepsilon^* \overrightarrow{E_m} \tag{3}$$

where $\overrightarrow{D_n}$ is the normal electric flux density, (C/m^2); $\overrightarrow{E_0}$ is the electric field intensity in the air gap, (V/m); ε^* is the relevant (to air) complex permittivity of the load, $\varepsilon^* = \varepsilon' - j\varepsilon''$, which leads to:

$$\overrightarrow{E_0} = (\varepsilon' - j\varepsilon'')\overrightarrow{E_m} \tag{4}$$

Since the bottom electrode is normally grounded, the voltage on the upper electrode is the total electric potential between the two electrodes (V), which can be divided into voltage falls in the air gap (V_0) and the voltage falls in food material (V_m):

$$V = V_0 + V_m = |\overrightarrow{E_0} d_0 + \overrightarrow{E_m} d_m| \tag{5}$$

Substitute Eqs. (4) into (5), it becomes:

$$|\overrightarrow{E_m}| = \frac{V}{\sqrt{(\varepsilon' d_0 + d_m)^2 + (\varepsilon'' d_0)^2}} \tag{6}$$

Then substitute Eqs. (6) back into (2) yields:

$$P = \rho c_p \frac{\partial T}{\partial t} = 2\pi f \varepsilon_0 \varepsilon'' |\overrightarrow{E_m}|^2 = 2\pi f \varepsilon_0 V^2 \frac{\varepsilon''}{(\varepsilon' d_0 + d_m)^2 + (\varepsilon'' d_0)^2} \tag{7}$$

or:

$$\frac{\partial T}{\partial t} = 2\pi f \varepsilon_0 V^2 \frac{\varepsilon''}{\rho c_p[(\varepsilon' d_0 + d_m)^2 + (\varepsilon'' d_0)^2]} \tag{8}$$

Accordingly, for linear temperature increases, the final temperature after processing can be described as:

$$T_f = T_i + t \cdot 2\pi f \varepsilon_0 V^2 \frac{\varepsilon''}{\rho c_p\left[(\varepsilon' d_0 + d_m)^2 + (\varepsilon'' d_0)^2\right]} \tag{9}$$

where T_f is the final temperature of load (°C), T_i is the initial temperature of load (°C), and t is the total processing time (s).

Metaxas (1996) studied the voltage across the load of a free-running oscillator RF system and found there is only a 7% variation between empty and full load in a typical industrial scale system. Therefore, it is a valid assumption that there is a constant voltage at the upper electrode for a certain product during RF heating. The assumption has been used in many previous researches (Marra et al., 2007; Birla et al., 2008a; Tiwari et al., 2011a,b). Since $2\pi f \varepsilon_0 V^2$ can be seen as a constant when the electrode gap is fixed, the heating rate only depends on the value of $\varepsilon''/\{\rho c_p[(\varepsilon' d_0 + d_m)^2 + (\varepsilon'' d_0)^2]\}$.

It can be seen from Eq. (8) that as the d_0 is reduced to zero, the value of ε' does not influence heating rate any more, which means that ε'' is the dominating factor in heat production. In this case, the heating mechanism changes from dielectric heating to resistive heating, in which the power conversion is dominated by the electric conductivity of the food (Metaxas, 1996):

$$P = 2\pi f \varepsilon_0 \varepsilon'' |E_m|^2 = \sigma |E_m|^2 \tag{10}$$

where $\sigma = 2\pi f\varepsilon_0\varepsilon''$, σ is the effective electric conductivity of the food load, (S/m).

However, d_0 is necessary in dielectric heating for in-package food heating in a continuous system. It can be found from Eq. (8) that as d_0 increases, the effect of ε' becomes significant. If all other parameters are considered as constant except for ε' and ε'', Eq. (8) can be seen as a binary function with ε' and ε'' as independent variables. But for a fixed ε'' value, the function becomes a monotonic decreasing function, which decreases with increasing ε'. Accordingly, for a fixed ε', the maximum result can be obtained as $\pi f\varepsilon_0 V^2/[\rho c_p(\varepsilon' + d_m/d_0)]$ when $\varepsilon'' = \varepsilon' + d_m/d_0$. Therefore, it can be concluded that when $\varepsilon'' < \varepsilon' + d_m/d_0$, an increase in ε'' will result in thermal runaway; but when $\varepsilon'' > \varepsilon' + d_m/d_0$, an increase in ε'' will reduce the heating rate. For most moist food, the ε' and ε'' are much larger than d_m/d_0 when d_0 and d_m are comparable. So the conclusion can be also written as: the maximum heating rate can be reached when $\varepsilon' \approx \varepsilon''$. This can be an approximate method for determining the heating rate trend by simply looking at dielectric properties of materials.

To validate the theoretical analysis over a wide range of dielectric properties, two representative foods were chosen for RF heating experiments: salty water and peanut butter. For salty water, the dielectric constant is relatively constant but loss factor changes largely with salt concentration; for peanut butter, both dielectric constant and loss factor change with varying moisture content and temperature. The dielectric properties and RF heating behaviors of the two materials would be adequate to validate the mathematical model. Furthermore, the two model foods were fed into different containers and treated with different electrode gaps in RF equipments to validate the high adaptability of the mathematical model.

2.2. Experiment validation I – salt solution

2.2.1. Sample preparation

A salt solution was prepared with table salt and double deionized water by controlling the weight percentage at 17 g/l (Sartorius BP 3100s, Data Weighing Systems Inc, IL, USA) and mixed evenly at room temperature. After an overnight stabilization, the solution was diluted to 9 different concentrations. The electric conductivity of each solution was measured by a bench conductivity meter (Con500, Cole Parmer, IL, USA). A standard curve of NaCl solution with different salt concentrations and electric conductivities was made (Fig. 2). Then solutions with electric conductivity of 0.03, 0.05, 0.1, 0.15, 0.2, 0.3, 0.5, 1, 2 and 3 S/m were selected and prepared to validate the model.

2.2.2. Properties of salt solution

Dielectric properties of the salt solutions with selected electrical conductivity were measured by an open-ended coaxial probe connected with an impedance analyzer (4291B, Agilent technologies Inc, Santa Clara CA, USA) at 22 °C over the frequency range of 10–1800 MHz. Prior to the measurement, the impedance analyzer was warmed up for 30 min before calibration to minimize system errors. Then the system was calibrated with open/short/low loss capacitance/50 Ω load in sequence, and the measuring probe was calibrated using air/short block/25 °C deionized water as recommended by the manufacturer. Software 85070D (Agilent Technologies, Inc., Santa Clara, CA, USA) was used to trigger the measurement and calculate the dielectric property. A cylinder sample holder (d = 20 mm, h = 94 mm) was designed to make sure the sample size satisfies the assumption of a semi-infinite body, which guarantees an accurate measurement (Feng et al., 2002). The sample holder was connected to an oil bath, which was used to bring the sample temperature up to 80 °C. After calibration, the salt solutions were poured into the sample holder one at a time, and the dielectric properties were measured. Between each measurement, both the probe and sample holder were cleaned with deionized water, dried and cooled down to room temperature. The detailed procedure and demonstrating scheme for dielectric property measurement can be found elsewhere (Wang et al., 2003a,c). Measurements were repeated twice for each sample.

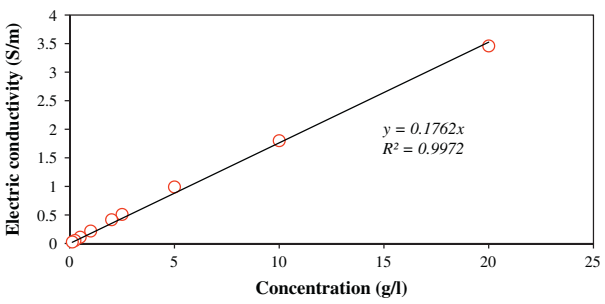

Fig. 2. Electrical conductivity regression curve for NaCl solutions with various salt concentrations.

2.2.3. RF heating test

The heating rate tests were conducted with a 6 kW, 27.12 MHz free-running oscillator RF system (COMBI 6-S, Strayfield International, Wokingham, UK). A detailed description of the RF heating system can be found elsewhere (Wang et al., 2010). A volume of 45 ml of each of the solutions with different concentrations was put into a 50 ml centrifuge tube (inner diameter d = 2.5 cm, h = 11.0 cm). The sample height was 9.5 cm (d_m) in the tube. The tube was placed vertically at the center of the bottom electrode. The gap between the electrode plates was fixed at 11 cm (air gap d_0 = 1.5 cm) for all tests so as to provide a reasonable comparison. A pre-calibrated fiber optical sensor (FOT-L, FISO, Quebec, Canada) was placed at the center of the sample for tracking temperature changes versus time (Fig. 3). The heating time was set for 3 min for all tests. Convective heat loss can be neglected because the sample containers were closed during treatment and there is no forced air flow during treatment.

2.3. Experiment validation II – peanut butter samples

2.3.1. Sample preparation

Commercial creamy peanut butter (IGA creamy peanut butter, IGA Inc, Chicago, IL, USA) was purchased from a local grocery store and stored at room temperature until use. The initial water content of the peanut butter was determined by the vacuum oven method (AOAC 925.40, 2010). Specifically, 2 g samples of peanut butter were weighed, transferred to aluminum dishes, spread evenly and heated in a vacuum oven (ADP-31, Yamato Scientific America Inc., Santa Clara, CA, USA) at 100 °C and 10 kPa. Samples were taken out and weighed every 1 h as drying continued, until the final weight change between the two consecutive measurements was less than 0.05 g/100 g. The samples were then cooled down in a desiccator for 30 min to room temperature, and then the final weights of the samples were measured by an analytical balance (Ohaus Analytical Plus, Ohaus Corporation, Florham Park, NJ,

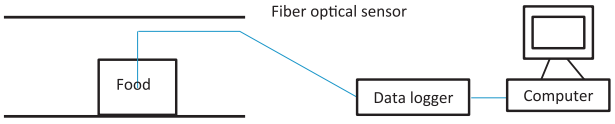

Fig. 3. Experimental setup for foods with a temperature measurement system in radio frequency heating.

USA). The experiment was conducted twice with 3 samples per batch, and water contents (wet basis) were calculated.

To prepare samples of higher moisture contents, pre-determined weights of deionized water were added into the commercial peanut butter samples and mixed by a hand mixer (Durabrand 5-speed hand mixer, Funai Electric Co., Ltd., Osaka, Japan) in a beaker (1 L) for 1 min to bring the moisture content of the peanut butter to 4%, 10%, 16% and 22% (w.b.), respectively. The minimal strength and time for blending were chosen to avoid generating heat and introducing air into the samples. The processed peanut butter samples were stored in air-tight glass containers at 4 °C for 24 h to allow the moisture to equilibrate, and mixed again at room temperature before taking measurements (AOAC 935.52, 2010). The moisture content of the conditioned samples was determined again by sampling from three random locations in the sample container to guarantee sample uniformity. The standard deviation of the tested moisture content was less than 0.5%.

2.3.2. Physical properties

The density of the original peanut butter sample was measured by the gravimetric method. An open-end metal cylinder tube with a known mass and volume (d = 5.0 cm, h = 1.0 cm) was used as a container for the volume measurement. Because of the high viscosity of the peanut butter, samples were heated up to 60 °C in a water bath (above melting point), and then filled into the metal cylinder tube. Precaution was taken to avoid air bubbles in the material during transfer. After the sample was cooled down to room temperature, both ends of the tube were scratched flat carefully. The total weight of the tube and sample were measured. The average density was calculated by dividing sample mass by sample volume. Measurements were made in three replicates.

Because of the difficulty in sample loading caused by the high viscosity of samples with higher water contents, the density of the peanut butter samples with water content 4%, 10%, 16% and 22% (w.b.) and temperature 20–80 °C were all obtained from Costherm® software (Aberdeen, UK). The prediction method in Costherm® is based on properties of composition of food materials and their change with temperature. It can be used for accurate predictions of most physical properties of food including initial freezing point, thermal conductivity, and heat capacity and enthalpy models to fat-containing foods with good accuracy and over an extended temperature range (Allen et al., 1997). The basic composition of food materials and the original density of peanut butter were also input as a reference for obtaining sample porosity for the determination of density with other moisture contents.

Heat capacity c_p (kJ/kg K) of peanut butter samples at different water contents was determined using a differential scanning calorimeter (DSC Q2000, TA Instruments, New Castle, DE, USA). An empty sealed aluminum pan was used as a reference and a 10–20 mg peanut butter samples was sealed in another aluminum pan (30 μl). The procedure included cooling the sample from room temperature to 0 °C at a ramping rate of 10 °C/min, equilibrating for 5 min, and then heating up to 80 °C. The measurements were made in three replicates.

Dielectric properties were measured using the same equipment and procedure as for the salt solution at 10–1800 MHz and 20–80 °C.

2.3.3. RF heating tests

The RF heater, temperature sensor and data logger used in this test were the same as for the salt solution test (Section 2.2.3). Rectangular polymeric trays (14.2 × 10.0 × 3.0 cm^3) were selected as the containers for peanut butter samples. Each individual peanut butter sample at different moisture contents was loaded into a polymeric tray with a thickness of 2 cm. The gap between the two electrodes was fixed at 10 cm to allow comparison for all samples, and the temperature sensor was kept in the center of the peanut butter tray to satisfy the one dimensional model. Each peanut butter sample was subjected to RF heating for 4 min for comparison.

To determine the temperature dependence, a peanut butter sample with 22% (w.b.) moisture content was placed into the same rectangular tray as mentioned and tested in the RF unit with an electrode gap of 13 cm and heating time of 48 min. The heating profile for each test was recorded by a data logger connected to the fiber optical temperature sensor (FOT-L, FISO, Quebec, Canada). This experiment was replicated twice.

3. Results and discussions

3.1. Salt solution – salt concentration dependence

The mean values of salt solution dielectric properties are summarized in Table 1. The thermal properties and density of all solutions were assumed to be the same as water since they were relatively stable with concentration change (c_p = 4.2 kJ/kg K, ρ = 1,000 kg/m^3). The anode current showing on the RF operating panel was constant for every solution at I = 0.42 A. The temperature–time profiles of the salt solutions during RF heating are shown in Fig. 4. It can be seen for all the tested solutions that the heating rate of the one with electric conductivity of 0.1 S/m was the highest (displayed by the dashed line). The heating rate of the solutions increased when the electric conductivity of the solution increased from 0.03 to 0.1 S/m. But then the heating rate decreased as the concentration increased from 0.1 to 3 S/m. Also, the temperature curves for the 0.03 and 0.05 S/m solutions are slightly non-linear, which is perhaps due to the temperature dependence of the dielectric properties. The heating rates of solutions with electrical conductivity higher than 0.1 S/m were relatively constant (not temperature sensitive).

By putting various properties into Eqs. (8) and (9), the heating rate and final temperature for 27.12 MHz were calculated. The top electrode voltage used in the prediction was 17,000 V according to the estimating equation (Birla et al., 2008a). The final temperature obtained from both Eq. (9) and experiment are shown in Fig. 5, in which the two curves correlated well. The discrepancy may come from the error of voltage estimation and deviations from the constant heating rate assumption for Eq. (9). The error may also be caused by the limitation of the one dimensional assumption in the theoretical model since the actual sample surface area was not as big as the electrodes. Although the tube has a relatively smaller geometry than the electrode, the predicted trend still followed well with experiment. This is because the discrepancy from one-dimensional assumption only caused the fringe field at the corners but will not influence the center temperature much.

Table 1
Dielectric properties (mean ± SD of two replicates) of NaCl solutions with 10 electric conductivities at 22 °C and 27.12 MHz.

Electrical conductivity (S/m)	Dielectric properties (–)	
	ε'	ε''
0.03	77.33 ± 0.12	18.12 ± 0.62
0.05	78.21 ± 0.93	30.47 ± 1.32
0.10	78.95 ± 0.57	36.18 ± 3.58
0.15	80.17 ± 0.81	64.93 ± 7.53
0.2	79.29 ± 0.13	119.24 ± 9.31
0.3	80.65 ± 1.03	155.99 ± 10.06
0.5	80.63 ± 0.27	277.99 ± 19.28
1	83.08 ± 0.84	573.45 ± 17.73
2	87.03 ± 0.43	1080.15 ± 23.41
3	91.56 ± 2.59	1577.03 ± 36.52

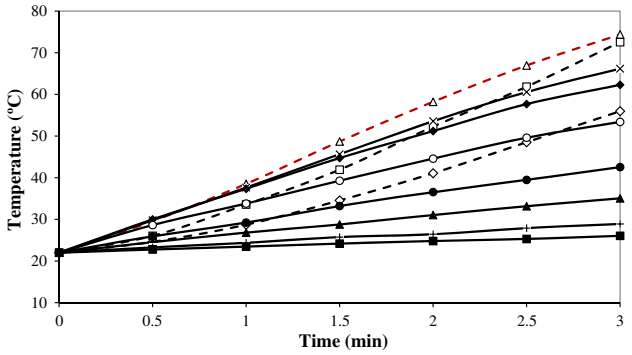

Fig. 4. Temperature–time histories for NaCl solutions with different electrical conductivity levels of 0.03 (◇), 0.05 (□), 0.1 (Δ), 0.15 (×), 0.2 (♦), 0.3 (○), 0.5 (●), 1 (▲), 2 (+) and 3 (■) S/m (dash for 0.03–0.1and bold for 0.15–3) subjected to RF heating at 27.12 MHz for 3 min (mean of 2 replicates).

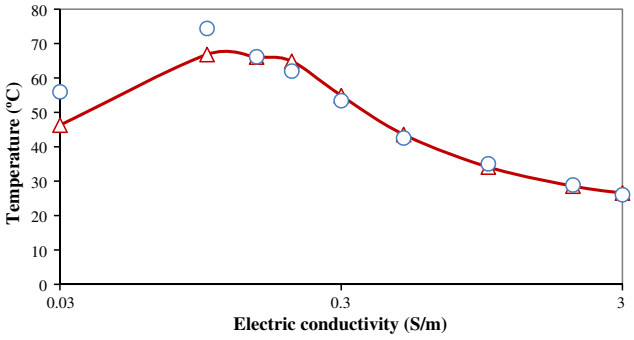

Fig. 5. Final temperatures after 3 min RF treatment of NaCl solutions with 10 different electric conductivities at 27.12 MHz obtained by theoretical prediction (Δ) and experiments (○).

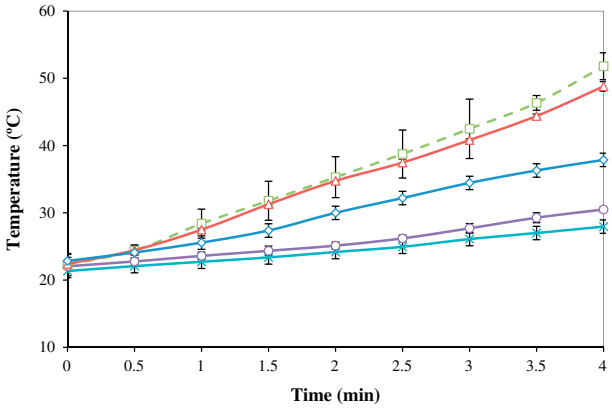

Fig. 6. Temperature–time histories for peanut butter with 5 moisture contents, 1.3% (×), 4% (○), 10% (□), 16% (Δ) and 22% (◊) w.b. during 4 min RF heating at 27.12 MHz.

3.2. Peanut butter

3.2.1. Moisture dependence

All the measured properties of peanut butter with various moisture contents are summarized in Table 2. The loss factor increased with increasing moisture content. This is possibly due to the fact that the salt dissolved more in the water as moisture content increased and formed more freely conductive ions. The electric current indicated on the RF machine operating panel varied from 0.52 to 0.60 A. Referring to the dielectric properties of peanut butter samples in Table 2, the loss factor ε'' was much smaller than the dielectric constant ε' at moisture content 1.3 and 4%, and ε'' was larger than ε' when moisture content was 22%. Thus, based on our earlier discussion, an approximate conclusion can be made that the maximum heating rate may happen in either 10% or 16% sample because the value of ε' and ε'' for those samples are more comparable.

The heating profile of peanut butter samples at various moisture contents is shown in Fig. 6. Within the 4 min heating period, all five heating curves were relatively linear, and the 10% sample had the highest heating rate (7.3 °C/min). Assuming the voltage at the upper electrode was 8500 V (Birla et al., 2008a; Tiwari et al., 2011b), the final temperatures obtained by both experiment and predicted methods are presented in Fig. 7. The estimated and experimental results agreed well, and the variation between the calculated and experimental values was less than 5 °C.

3.2.2. Temperature dependence

From the dielectric properties for 22% (w.b.) moisture content peanut butter sample in Table 2, it can be observed that $\varepsilon'' > \varepsilon'$ at room temperature, and ε'' increased faster than ε' as the temperature increased. This trend may lead to a decreasing heating rate as discussed previously in the calculation in Section 2.1. The temperature–time curve for the peanut butter sample with 22% (w.b.)

Table 2
Properties of peanut butter with 5 selected moisture content levels at temperature 20–80 °C and 27.12 MHz (dielectric properties presented in mean ± SD of two replicates).

Moisture content (w.b.) (%)		1.3	4	10	16	22
Density (kg/m^3)		1115.1	1111.9	1104.8	1097.7	1090.6
Heat capacity (kJ/kg K)		2.03	2.17	2.45	2.67	2.91
Dielectric constant (ε')	20 °C	3.26 ± 0.01	3.40 ± 0.28	6.77 ± 0.17	13.12 ± 1.79	18.25 ± 1.24
	30 °C	3.32 ± 0.03	3.51 ± 0.32	6.92 ± 0.08	14.12 ± 1.06	20.01 ± 0.78
	40 °C	3.39 ± 0.02	3.62 ± 0.32	7.26 ± 0.18	15.02 ± 0.81	23.66 ± 0.46
	50 °C	3.43 ± 0.01	3.74 ± 0.35	7.52 ± 0.64	16.74 ± 1.89	26.20 ± 0.93
	60 °C	3.48 ± 0.01	3.81 ± 0.54	8.01 ± 1.11	20.86 ± 0.45	30.89 ± 3.54
	70 °C	3.52 ± 0.01	3.87 ± 0.69	8.12 ± 2.36	24.95 ± 2.11	39.52 ± 1.70
	80 °C	3.58 ± 0.01	3.95 ± 0.87	8.85 ± 2.01	29.26 ± 3.74	54.22 ± 3.60
Loss factor (ε'')	20 °C	0.09 ± 0.03	0.10 ± 0.02	1.72 ± 0.16	8.30 ± 2.62	27.51 ± 1.82
	30 °C	0.08 ± 0.02	0.10 ± 0.02	1.89 ± 0.12	9.25 ± 1.50	36.35 ± 4.20
	40 °C	0.07 ± 0.01	0.12 ± 0.02	2.15 ± 0.05	10.51 ± 1.27	65.77 ± 0.08
	50 °C	0.07 ± 0.02	0.14 ± 0.02	2.37 ± 0.38	11.96 ± 0.78	83.23 ± 4.87
	60 °C	0.06 ± 0.02	0.14 ± 0.01	2.97 ± 0.54	20.40 ± 4.65	114.68 ± 9.88
	70 °C	0.05 ± 0.01	0.15 ± 0.04	3.51 ± 1.08	29.81 ± 10.82	172.10 ± 42.63
	80 °C	0.04 ± 0.01	0.18 ± 0.06	4.14 ± 0.52	40.03 ± 17.35	278.67 ± 63.73

moisture content over a 48 min heating period in RF system is shown in Fig. 8. As the temperature increased with time, the heating rate decreased, which supported the theoretical prediction.

To further analyze the trend, the heating rate versus temperature is plotted in Fig. 9(a). The coefficient $\varepsilon''/\{\rho c_p[(\varepsilon' d_0 + d_m)^2 + (\varepsilon'' d_0)^2]\}$ is calculated and plotted versus temperature in Fig. 9(b). Comparing (a) and (b), the trends correlate well. Similar trends can also be found in Wang et al. (2003a) for the heating rate of codling moth slurry and gellan gel, which has a loss factor larger than the dielectric constant, and increases much faster than dielectric constant.

3.2.3. Determination of heating rate from dielectric properties plot

According to the calculation discussed above (Section 2.1), a method to estimate the heating rate of samples in this study is to plot the dielectric constant versus loss factor (Fig. 10). A $y = x$ is also plotted as a reference for the comparison of dielectric constant and loss factor. The closer the data points approached $y = x$, the higher heating rate can be achieved based on the theoretical calculations.

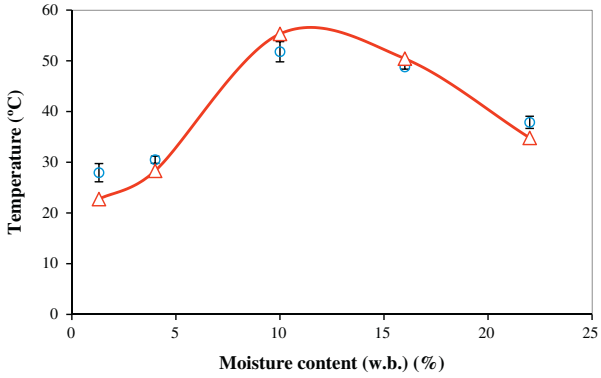

Fig. 7. Final temperature comparison of peanut butter samples with five water contents after 4 min RF heating at 27.12 MHz between experiments (○) and prediction (△).

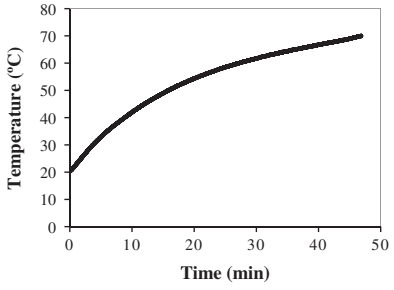

Fig. 8. Time–temperature curve for peanut butter with 22% (w.b.) moisture content with 48 min 27.12 MHz RF heating (mean of 2 replicates).

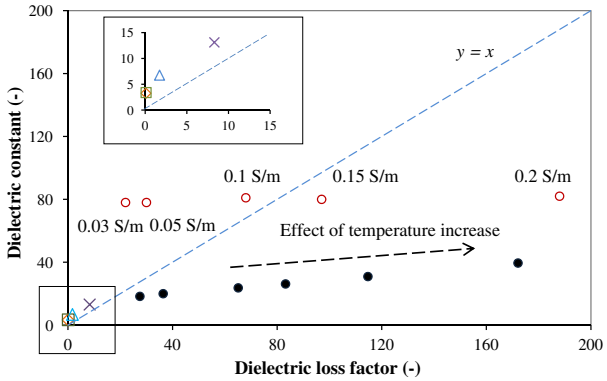

Fig. 10. Dielectric properties of peanut butter samples (pb 1.3% (◊), 4% (□), 10% (△), 16% (×) at room temperature, 22% (●) at 20–70 °C) and salty water (electric conductivity 0.03–0.2 S/m (○) at room temperature) with a function curve of $y = x$ at 27.12 MHz for estimating the maximum heating rate.

For peanut butter samples except the one with 22% (w.b.) moisture content, it is difficult to tell which one may have a higher heating rate from the graph since they are all close to the $y = x$ curve. In this situation, a specific analysis needs to be conducted as mentioned in the results section. The temperature dependent dielectric properties of the 22% (w.b.) sample showed that the data point was leaving the $y = x$ as temperature increased. This trend agreed with the experiment results in Fig. 9. For salt solution samples, the data points showed the highest heating rate happened between 0.1 and 0.15 S/m, which approximately agreed with Fig. 4. The specific heating rate comparison can be found through the mathematical model.

4. Conclusions

A mathematical equation was deduced to better understand the heating behavior of food products in RF heating. Dielectric properties were found as the major factor affecting the heating rate in RF systems with a fixed electrode gap. The properties of salt solutions and peanut butter samples were obtained as the input parameters for the mathematical model to predict the RF heating behavior. It was found from the model that with a certain air gap and material thickness that the closer ε'' approaches ε', the higher heating rate of which can be obtained. The experimental results showed that dielectric properties influenced the heating behavior in a free-running oscillator RF system in a predictable manner. The results with two food samples, salt solution and peanut butter with adjusted

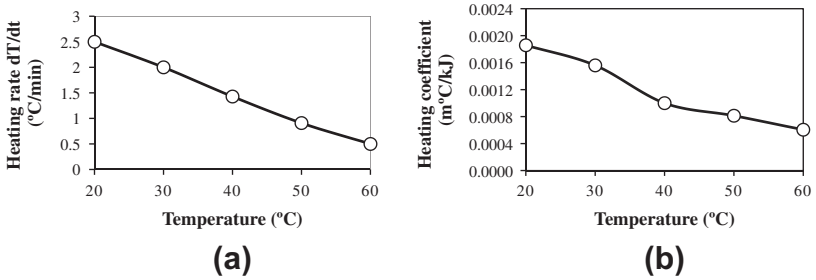

Fig. 9. Tendency comparison between experimental heating rate for a 48 min RF heating at 27.12 MHz (a) and heating rate coefficient $\varepsilon''/\{\rho c_p[(\varepsilon' d_0 + d_m)^2 + (\varepsilon'' d_0)^2]\}$ (b) calculated from the dielectric properties of peanut butter with 22% (w.b.) moisture content.

moisture contents, indicated that the heating rate can be predicted by the mathematical model with varying dielectric properties in a large range and various RF heating conditions. That is, when the value of ε' was closer to ε'', the heating rate was the highest. This conclusion may contribute to a better understanding as to how heating rate is influenced by food properties in a RF system with free-running oscillator.

Acknowledgements

This research was conducted in the Department of Biological Systems Engineering, Washington State University (WSU), supported by grants from WSU Agricultural Research Center, and from USDA-NIFA-NIFSI (2011-51110-30994 and 2012-67005-19598). The author thanks Drs. Roopesh Mohandas and Shyam Sablani for providing the help in heat capacity measurement with differential scanning calorimetry. The authors also thank the China Scholarship Council for the scholarship to Yang Jiao for her Ph.D study.

References

Allen, A.R., Liu, M. and Nesvadba, P., 1997. Development of integrated software for the modeling of thermal processing of foods. In: Proceedings of the conference, Modeling of thermal properties and behaviour of foods during production, storage and distribution, Prague.

Birla, S.L., Wang, S., Tang, J., 2008a. Computer simulation of radio frequency heating of model fruit immersed in water. Journal of Food Engineering 84 (2), 270–280.

Birla, S.L., Wang, S., Tang, J., Tiwari, G., 2008b. Characterization of radio frequency heating of fresh fruits influenced by dielectric properties. Journal of Food Engineering 89 (4), 390–398.

Calay, R.K., Newborough, M., Probert, D., Calay, P.S., 1994. Predictive equations for the dielectric-properties of foods. International Journal of Food Science and Technology 29 (6), 699–713.

Choi, C.T.M., Konrad, A., 1991. Finite-element modeling of the Rf heating process. Ieee Transactions on Magnetics 27 (5), 4227–4230.

Farag, K.W., Lyng, J.G., Morgan, D.J., Cronin, D.A., 2011. A comparison of conventional and radio frequency thawing of beef meats: effects on product temperature distribution. Food and Bioprocess Technology 4 (7), 1128–1136.

Feng, H., Tang, J., Cavalieri, R.P., 2002. Dielectric properties of dehydrated apples as affected by moisture and temperature. Transactions of the ASAE 45 (1), 129–135.

Gao, M., Tang, J., Villa-Rojas, R., Wang, Y., Wang, S., 2011. Pasteurization process development for controlling Salmonella in in-shell almonds using radio frequency energy. Journal of Food Engineering 104 (2), 299–306.

Guo, Q., Piyasena, P., Mittal, G.S., Si, W., Gong, J., 2006. Efficacy of radio frequency cooking in the reduction of Escherichia coli and shelf stability of ground beef. Food Microbiology 23 (2), 112–118.

Jones, P.L., Rowley, A.T., 1996. Dielectric drying. Drying Technology 14 (5), 1063–1098.

Luechapattanaporn, K. et al., 2005. Sterilization of scrambled eggs in military polymeric trays by radio frequency energy. Journal of Food Science 70 (4), E288–E294.

Manzocco, L., Anese, M., Nicoli, M.C., 2008. Radiofrequency inactivation of oxidative food enzymes in model systems and apple derivatives. Food Research International 41 (10), 1044–1049.

Marra, F., Lyng, J., Romano, V., McKenna, B., 2007. Radio-frequency heating of foodstuff: solution and validation of a mathematical model. Journal of Food Engineering 79 (3), 998–1006.

Metaxas, A.C., 1996. Foundations of Electroheat: a Unified Approach. Wiley.

Nelson, S.O., 1981. Review of factors influencing the dielectric properties of cereal grains. Cereal Chemistry 58 (6), 487–492.

Palazoglu, T.K., Coskun, Y., Kocadagli, T., Gokmen, V., 2012. Effect of radio frequency postdrying of partially baked cookies on acrylamide content, texture, and color of the final product. Journal of Food Science 77 (5), E113–E117.

Piyasena, P., Dussault, C., Koutchma, T., Ramaswamy, H.S., Awuah, G.B., 2003. Radio frequency heating of foods: principles, applications and related properties – a review. Critical Reviews in Food Science and Nutrition 43 (6), 587–606.

Rice, J., 1993. RF technology sharpens bakery's competitive edge. Food Processing 6, 18–24.

Rowley, A.T., 2001. Radio frequency heating. In: Richardson, P. (Ed.), Thermal Technologies in Food Processing. Woodhead Publishing Cambridge, Cambridge, UK, pp. 127–162.

Sosa-Morales, M.E., Valerio-Junco, L., Lopez-Malo, A., Garcia, H.S., 2010. Dielectric properties of foods: reported data in the 21st Century and their potential applications. LWT-Food Science and Technology 43 (8), 1169–1179.

Tiwari, G., Wang, S., Tang, J., Birla, S.L., 2011a. Analysis of radio frequency (RF) power distribution in dry food materials. Journal of Food Engineering 104 (4), 548–556.

Tiwari, G., Wang, S., Tang, J., Birla, S.L., 2011b. Computer simulation model development and validation for radio frequency (RF) heating of dry food materials. Journal of Food Engineering 105 (1), 48–55.

To, E.C., Mudgett, R.E., Wang, D.I.C., Goldblith, S.A., Decareau, R.V., 1974. Dielectric properties of food materials. Journal of Microwave Power 9 (4), 303–315.

Wang, J., Olsen, R.G., Tang, J., Tang, Z., 2008. Influence of mashed potato dielectric properties and circulating water electric conductivity on radio frequency heating at 27 MHz. Journal of Microwave Power and Electromagnetic Energy 42 (2), 31–46.

Wang, S., Tang, J., 2001. Radio frequency and microwave alternative treatments for insect control in nuts: a review. Agricultural Engineering Journal 10 (3&4), 105–120.

Wang, S., Tang, J., Cavalieri, R.P., Davies, D.C., 2003a. Differential heating of insects in dried nuts and fruits associated with radio frequency and microwave treatments. Transactions of the ASAE 46 (4), 1175–1182.

Wang, S., Tiwari, G., Jiao, S., Johnson, J.A., Tang, J., 2010. Developing postharvest disinfestation treatments for legumes using radio frequency energy. Biosystems Engineering 105 (3), 341–349.

Wang, Y., Wig, T.D., Tang, J., Hallberg, L.M., 2003b. Sterilization of foodstuffs using radio frequency heating. Journal of Food Science 68 (2), 539–544.

Wang, Y., Wig, T.D., Tang, J., Hallberg, L.M., 2003c. Dielectric properties of foods relevant to RF and microwave pasteurization and sterilization. Journal of Food Engineering 57 (3), 257–268.